



Growth of [110] $\text{La}_{2/3}\text{Sr}_{1/3}\text{MnO}_3 - \text{YBa}_2\text{Cu}_3\text{O}_7$ heterostructures

Soumen Mandal, Saurabh K. Bose, Rajeev Sharma, R. C. Budhani, Prahallad Padhan, and Wilfrid Prellier

Citation: *Applied Physics Letters* **89**, 182508 (2006); doi: 10.1063/1.2374692

View online: <http://dx.doi.org/10.1063/1.2374692>

View Table of Contents: <http://scitation.aip.org/content/aip/journal/apl/89/18?ver=pdfcov>

Published by the [AIP Publishing](#)



Re-register for Table of Content Alerts

Create a profile.



Sign up today!



Growth of [110] $\text{La}_{2/3}\text{Sr}_{1/3}\text{MnO}_3$ - $\text{YBa}_2\text{Cu}_3\text{O}_7$ heterostructures

Soumen Mandal, Saurabh K. Bose, Rajeev Sharma, and R. C. Budhani^{a)}
 Department of Physics, Indian Institute of Technology Kanpur, Kanpur 208016, India

Prahallad Padhan and Wilfrid Prellier
 Laboratoire CRISMAT, CNRS UMR 6508, ENSICAEN, 6 Bd. du Marechal Juin,
 F-14050 Caen Cedex, France

(Received 5 July 2006; accepted 18 September 2006; published online 1 November 2006)

$\text{YBa}_2\text{Cu}_3\text{O}_7$ - $\text{La}_{2/3}\text{Sr}_{1/3}\text{MnO}_3$ heterostructures of [110] orientation are grown to allow direct injection of spin polarized holes from the $\text{La}_{2/3}\text{Sr}_{1/3}\text{MnO}_3$ into the CuO_2 superconducting planes. The magnetic response of the structure at $T < T_{\text{sc}}$ shows both diamagnetic and ferromagnetic moments with [001] direction as magnetic easy axis. While the superconducting transition temperature (T_{sc}) of these structures is sharp ($\Delta T_{\text{sc}} \approx 2.5$ K), the critical current density (J_c) follows a dependence of the type $J_c = J_0(1 - T/T_{\text{sc}})^{3/2}$ with highly suppressed $J_0 (\approx 2 \times 10^4 \text{ A/cm}^2)$, indicating strong pair breaking effects of the ferromagnetic boundary. © 2006 American Institute of Physics. [DOI: 10.1063/1.2374692]

The transport of quasiparticles and paired electrons across superconductor (SC)-ferromagnet (FM) proximity effect junctions provides valuable information on the degree of spin polarization in the ferromagnet, exchange-field-induced inhomogeneous superconductivity at the SC-FM interface, symmetry of the SC order parameter, and a plethora of other effects arising from the antagonism between superconductivity and ferromagnetism,¹⁻³ some of which are technologically important.^{4,5} There have been extensive studies of polarized and unpolarized quasiparticle injection in conventional *s*-wave superconductors.^{1,2,6} Similar investigations in heterostructures of ferromagnetic manganites and hole doped cuprates present a rich field of research due to the *d*-wave symmetry of the SC order parameter and a high degree of spin polarization in manganites. One of the systems of interest for such studies is $\text{YBa}_2\text{Cu}_3\text{O}_7$ - $\text{La}_{2/3}\text{Sr}_{1/3}\text{MnO}_3$ - $\text{YBa}_2\text{Cu}_3\text{O}_7$ (YBCO-LSMO-YBCO) trilayer. While magnetotransport and magnetic ordering in such manganite-cuprate heterostructures and superlattices have been studied in detail,⁷⁻¹⁰ the YBCO in all such studies has *c* axis perpendicular to the plane of the substrate. Since superconductivity in YBCO lies in the CuO_2 planes (*ab* plane), the *c*-axis oriented structure does not allow injection of quasiparticles along the nodal or fully gapped directions of the Fermi surface. In order to overcome this difficulty, it is necessary to grow the YBCO layer with crystallographic orientation such that the CuO_2 planes are normal to the substrate. This can be achieved by growing either [100]/[010] or [110] oriented YBCO films. While the [100]/[010] and [110] YBCO oriented films on lattice matched substrates have been deposited successfully,¹¹⁻¹³ the growth of a FM-SC heterostructure or superlattice with the CuO_2 planes normal to the plane of the substrate is quite nontrivial.

In this work we report the growth of [110] oriented LSMO-YBCO heterostructures on [110] SrTiO_3 (STO) which had a 500 Å $\text{PrBa}_2\text{Cu}_3\text{O}_7$ (PBCO) template. The SC heterostructures show in plane magnetic anisotropy with [001] as the magnetic easy axis and clear diamagnetic and

ferromagnetic contributions to hysteresis at $T < T_{\text{sc}}$.

Thin films of PBCO-LSMO-YBCO were deposited using pulsed laser ablation technique.¹⁰ The optimized growth temperature (T_d), oxygen partial pressure p_{O_2} , laser energy density (E_d), and growth rate (G_r) used for the deposition of the 500 Å thick PBCO template were, 700 °C, 0.4 mbar, $\sim 2 \text{ J/cm}^2$, and 1.6 Å/s, respectively. After the deposition of the PBCO layer the substrate temperature was raised to 750 °C keeping the p_{O_2} constant. The growth of 300 Å thick LSMO was carried out at $T_d = 750$ °C, $p_{\text{O}_2} = 0.4$ mbar, $E_d \sim 2 \text{ J/cm}^2$, and $G_r \approx 0.5$ Å/s. Once the growth of the LSMO layer was complete, a 1000 Å YBCO film was deposited on top of the PBCO-LSMO bilayer at $T_d = 800$ °C, $p_{\text{O}_2} = 0.4$ mbar, $E_d \sim 2 \text{ J/cm}^2$, and $G_r \approx 1.6$ Å/s. After completion of this layer, the deposition chamber was filled with O_2 to atmospheric pressure and then the sample was cooled to room temperature with a 30 min holdup at 500 °C to realize full oxygenation of the structure. These deposition parameters were established after taking a series of calibration runs where the crystal orientation, high T_{sc} of the YBCO, and low coercivity (H_c) of the LSMO layer were important factors in deciding the best condition.

In Fig. 1 we have shown θ - 2θ scans of a PBCO-LSMO-YBCO heterostructure. Two intense doublets located at $2\theta \approx 32.5^\circ$ and 69° are seen of which the lower angle component is due to the [110] and [220] reflections of the substrate. The weaker component of the doublets which appears at

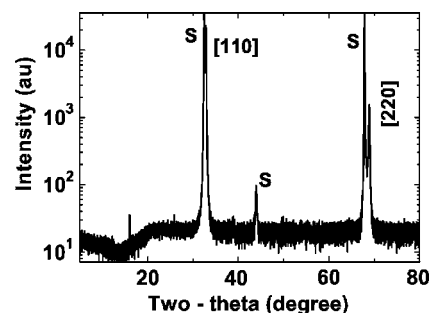


FIG. 1. θ - 2θ x-ray diffraction pattern of PBCO-LSMO-YBCO heterostructure grown on [110] STO.

^{a)}Electronic mail: reb@iitk.ac.in

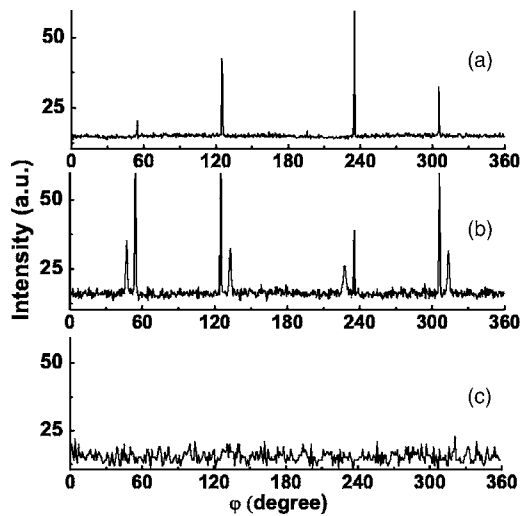


FIG. 2. ϕ scans of the PBCO-LSMO-YBCO heterostructure. Panels (a) and (b) show the [117] ϕ scan for [110] and [103] phases, respectively, clearly indicating the presence of both [103]/[110] phases of YBCO. Panel (c) shows the [109] ϕ scan for the [001] phase, indicating the absence of the same.

higher 2θ is identified with the scattering vector of the heterostructure normal to the plane of the substrate. However, the observations of these peaks in θ - 2θ scattering geometry does not confirm [110] phase purity as the reflections from [103] and [013] oriented phases also fall at the same 2θ value. Figure 2 panels (a), (b), and (c) respectively show the ϕ scans of [117] peak from [110] and [103] phases of YBCO and [109] ϕ scan for [001] phase of YBCO. In panel (a) we see four peaks while panel (b) shows eight. This is due to the fact that the [117] peaks from the [110] phase of YBCO and LSMO lie at the same position while this is not the case when we are probing the [117] peaks from the [103] oriented phase. The absence of any peak in panel (c) rules out the [001] phase. The volume percentage of [110] oriented grains calculated from the recipe of Westerheim *et al.*¹⁴ comes out to be $\geq 65\%$ with the remaining volume of [103] grains. While the growth is not 100% [110] oriented, the remaining [103] grains still permit injection of spin polarized carriers directly into the CuO_2 planes as these planes are oriented at 45° with respect to the substrate.

In Fig. 3 we have shown M vs H loops for a PBCO-

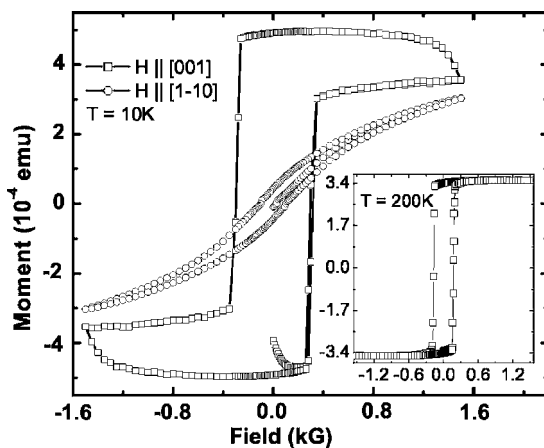


FIG. 3. M vs H loops for PBCO-LSMO-YBCO heterostructures taken at 10 K with field parallel and perpendicular to the $[1\bar{1}0]$ substrate edge. The inset shows the M - H loop with H along the magnetic easy axis at 200 K.

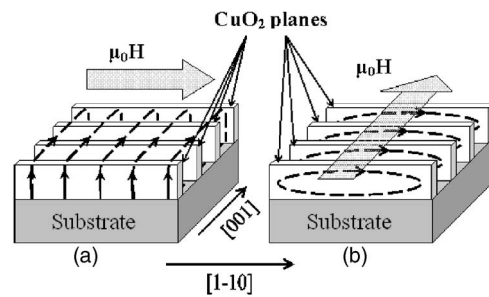


FIG. 4. (a) Josephson tunneling controlled screening current in [110] oriented heterostructure when the applied field H is parallel to CuO_2 planes. (b) In-plane screening current in [110] oriented heterostructure when the applied field H is perpendicular to CuO_2 planes.

LSMO-YBCO heterostructure taken at 10 K with field H parallel to $[001]$ and $[1\bar{1}0]$ directions of the substrate. The square hysteresis loop in the main figure (and in the inset) when $H \parallel [001]$ as against a slowly saturating loop when $H \parallel [1\bar{1}0]$ clearly shows that $[001]$ is the magnetic easy axis of the LSMO. We can also see distinctly the diamagnetic contribution from the SC, which splits the field increasing and field decreasing arms of the loop beyond the saturation field. This splitting is because of the SC state confirmed by the absence of the same in the M - H loop taken at 200 K (inset). A calculation of the critical current density (J_c) from the shift of M - H loop using the Bean model¹⁵ yields $J_c \approx 3.8 \times 10^4$ A/cm² at 10 K and 350 G field. A remarkable feature of these hysteresis loops is the near absence of the diamagnetic contribution when the magnetic field is aligned along the magnetic hard axis ($[1\bar{1}0]$) of LSMO. These features can be understood if we visualize the way screening currents are induced in the SC film by the external field. As shown in Fig. 4, when the external field is parallel to CuO_2 planes ($H \parallel [1\bar{1}0]$), the diamagnetic moment is produced by weak Josephson tunneling currents across the CuO_2 planes. However, for $H \parallel [001]$, the screening currents are confined to each CuO_2 plane. A large condensate density in the planes makes these currents strong and the diamagnetic moment is distinctly visible in the M - H loop. The hysteresis loop

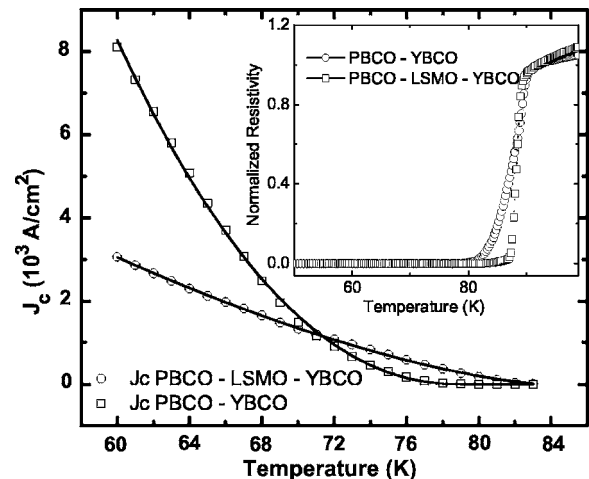


FIG. 5. Transport $J_c(T)$ data for PBCO-YBCO and PBCO-LSMO-YBCO heterostructures taken with voltage criterion of 10 $\mu\text{V}/\text{cm}$. The solid lines are the fitting using the formula $J_c = J_{c0}(1 - T/T_c)^\beta$. The inset shows the resistivity of the same samples in the vicinity of the T_c . The resistivity has been normalized with respect to its value at 92 K.

shift due to superconductivity in $\text{La}_{0.7}\text{Ca}_{0.3}\text{MnO}_3$ -YBCO- $\text{La}_{0.7}\text{Ca}_{0.3}\text{MnO}_3$ superlattices have been reported by Peña *et al.*⁹ Their calculation of J_c on the basis of the Bean model yields a suppression of the current by a factor of 20 at 5 K. However, the work in Ref. 9 is on c -axis oriented films, where the suppression of the J_c due to ferromagnetic proximity effect may be small as the c -axis coherence length ξ_c of YBCO is only ≈ 3 Å.

In Fig. 5 we have shown the variation of transport J_c with temperature for PBCO-LSMO-YBCO (circle) and PBCO-YBCO (square) heterostructures where PBCO is 500 Å, LSMO is 300 Å, and YBCO is 2000 Å thick, the LSMO layer being absent in the second structure while other thicknesses are same. The SC transition in these samples measured in a four-probe geometry is shown in the inset of Fig. 5. We note that while this transition in PBCO-LSMO-YBCO heterostructure is quite sharp ($\Delta T_{sc} \approx 2.5$ K) as compared to the [110] oriented PBCO-YBCO bilayer, its J_c is greatly suppressed. The $J_c(T)$ data have been fitted to the phenomenological relation $J_c = J_o(1 - T/T_{sc})^\beta$. The fitting parameters for PBCO-LSMO-YBCO and PBCO-YBCO structures are $J_o = 2.0 \times 10^4$ and 1.8×10^5 A/cm², respectively, while $\beta = 1.5$ and 2.16, respectively. In the Ginzburg-Landau description of $J_c(T)$ the prefactor J_o is directly related to the condensate density. A highly suppressed J_o in samples with ferromagnetic boundary provides a strong indication of pair breaking by spin polarized carriers injected from the LSMO.

In summary, manganite-cuprate bilayers where CuO_2 planes are normal to the plane of the templated [110] SrTiO_3 have been synthesized. This structure is amenable to deposi-

tion of a second low-coercivity LSMO film on top of the YBCO. Studies of the ferromagnetism and superconductivity in such [110] oriented FM-SC-FM structures are in progress.

The authors acknowledge financial support from the Indo-French Center for Promotion of Advanced Research and the Department of Defence, Government of India.

¹A. I. Buzdin, Rev. Mod. Phys. **77**, 935 (2005).

²I. F. Lyuksyutov and V. L. Pokrovsky, Adv. Phys. **54**, 67 (2005).

³F. S. Bergeret, A. F. Volkov, and K. B. Efetov, Rev. Mod. Phys. **77**, 1321 (2005).

⁴J. Y. Gu, C.-Y. You, J. S. Jiang, J. Pearson, Ya. B. Bazaliy, and S. D. Bader, Phys. Rev. Lett. **89**, 267001 (2002).

⁵J. Eom and Mark Johnson, Appl. Phys. Lett. **79**, 2486 (2001).

⁶R. Meservey and P. M. Tedrow, Phys. Rep. **238**, 173 (1994).

⁷A. M. Goldman, V. Vas'ko, P. Kraus, K. Nikolaev, and V. A. Larkin, J. Magn. Magn. Mater. **200**, 69 (1999).

⁸Z. W. Dong, R. Ramesh, T. Venkatesan, Mark Johnson, Z. Y. Chen, S. P. Pai, V. Talyansky, R. P. Sharma, R. Shreekala, C. J. Lobb, and R. L. Greene, Appl. Phys. Lett. **71**, 1718 (1997).

⁹V. Peña, Z. Sefrioui, D. Arias, C. Leon, J. Santamaria, M. Varela, S. J. Pennycook, and J. L. Martinez, Phys. Rev. B **69**, 224502 (2004).

¹⁰K. Senapati and R. C. Budhani, Phys. Rev. B **71**, 224507 (2005).

¹¹C. B. Eom, A. F. Marshall, S. S. Laderman, R. D. Jacowitz, and T. H. Geballe, Science **249**, 1549 (1990).

¹²A. Inam, C. T. Rogers, R. Ramesh, K. Remschnig, L. Farrow, D. Hart, T. Venkatesan, and B. Wilkens, Appl. Phys. Lett. **57**, 2484 (1990).

¹³M. Covington, R. Scheuerer, K. Bloom, and L. H. Greene, Appl. Phys. Lett. **68**, 1717 (1996).

¹⁴A. C. Westerheim, Alfredo C. Anderson, D. E. Oates, S. N. Basu, D. Bhatt, and M. J. Cima, J. Appl. Phys. **75**, 393 (1994).

¹⁵J. H. Classen, in *Magnetic Susceptibility of Superconductors and Other Spin Systems*, edited by R. A. Hein, T. L. Francavilla, and D. H. Liebenberg (Plenum, New York, 1991), p. 405.